Supporting Information

Fe_2P nanoparticles-decorated carbon nanofiber composite towards lightweight and highly-efficient microwave absorption

Yao Li [a], Guangguang Guan [a], Liang Yan [a], Kaiyin Zhang [b] and Jun Xiang *[a]

[a] *School of Science, Jiangsu University of Science and Technology, Zhenjiang 212100, PR China*

[b] *College of mechanical and electrical engineering, Wuyi University, Wuyishan 354300, PR China*

**Corresponding author.*

E-mail address: jxiang@just.edu.cn (J. Xiang)

Experimental section

1. Materials

Polyacrylonitrile (PAN, Mw = 150,000), N.N-Dimethylformamide (DMF), ferric acetylacetonate ($Fe(acac)_3$), and phosphornitrilic chloride trimer ($Cl_6N_3P_3$) were purchased from Shanghai Aladdin Biochemical Technology Co., Ltd. All the materials were used directly without further purification.

2. Characterization

Phase structure of Fe_2P@CNFs and CNFs were analyzed by X-ray diffractometer (XRD, Shimadzu XRD-6000) with Cu Kα radiation (λ = 0.15406 nm). Raman spectra were recorded on a Renishaw in Via Reflex Raman spectrometer with a 532 nm laser. The surface morphology and microstructure of the samples were observed through field-emission scanning electron microscopy (FE-SEM, Zeiss Merlin Compact) and transmission electron microscope (TEM, FEI Tecnai F20 G2). Thermogravimetric (TG) analysis was conducted on a Shimadzu DTG-60H thermal analyzer from room temperature to 800 °C with a heating rate of 10 °C/min in air atmosphere.

3. Electromagnetic measurement

To investigate the electromagnetic characteristics and microwave absorption properties, the prepared products were uniformly mixed with paraffin wax at a mass ratio of 1:9 (10 wt%), and then pressed into toroidal-shaped specimens with an outer diameter of 7.00 mm, an inner diameter of 3.04 mm, and a thickness of 2–3 mm. The vector network analyzer (Agilent PAN N5224A) was employed to measure the electromagnetic parameters in the frequency range of 2–18 GHz based on a coaxial transmission/reflection mode. To reveal the effect of the filling ratio on the EM and MA performances,

the composites with 7.5 wt% and 12.5 wt% Fe_2P@CNFs were also prepared.

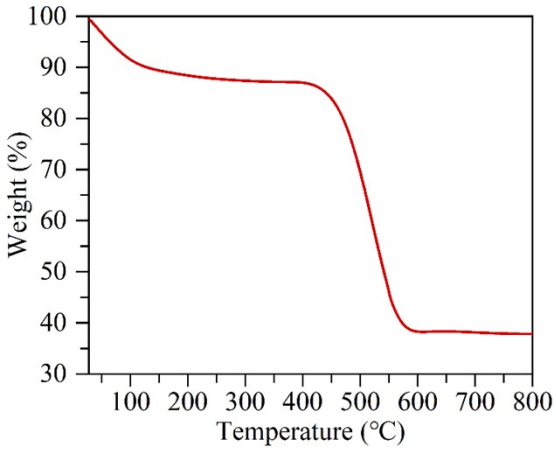

Fig. S1 TG curve of Fe_2P@CNFs.

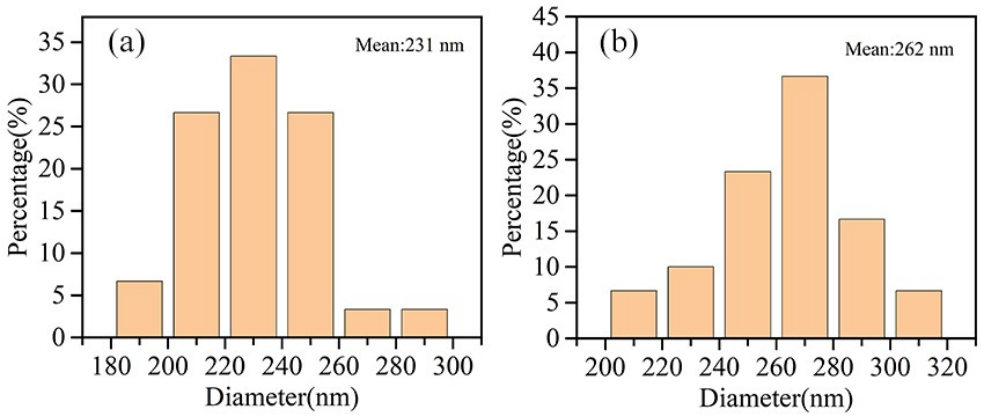

Fig. S2 Diameter distribution diagrams of (a) CNFs and (b) Fe_2P@CNFs.

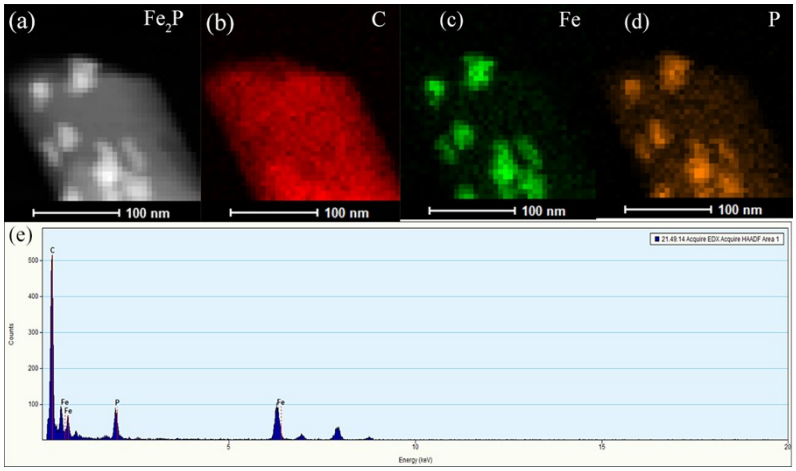

Fig. S3 HAADF-STEM image and corresponding elemental mappings of Fe_2P@CNFs

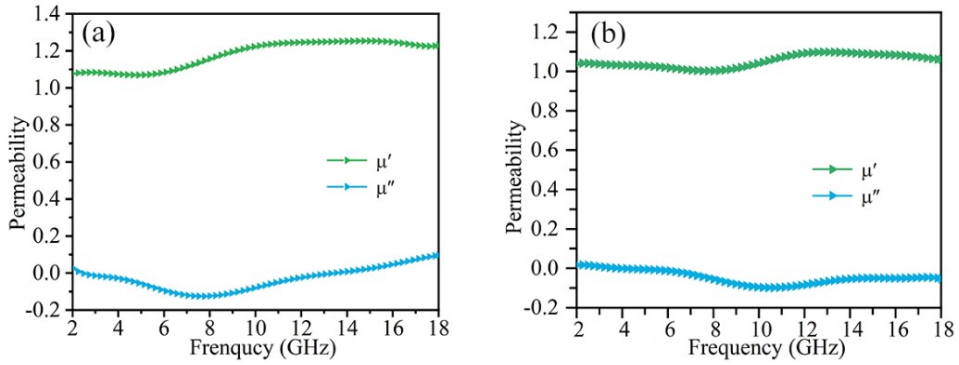

Fig. S4 Frequency dependence of relative complex permeability for (a) CNFs and (b) Fe_2P@CNFs.

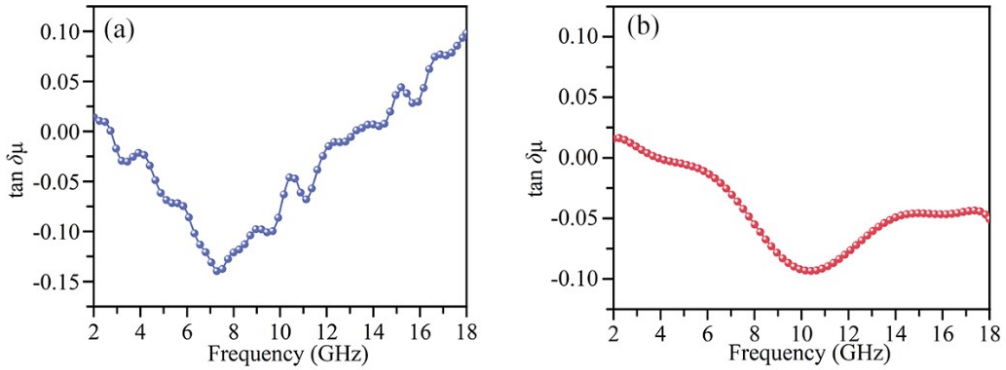

Fig. S5 Magnetic loss tangents of CNFs and Fe_2P@CNFs.

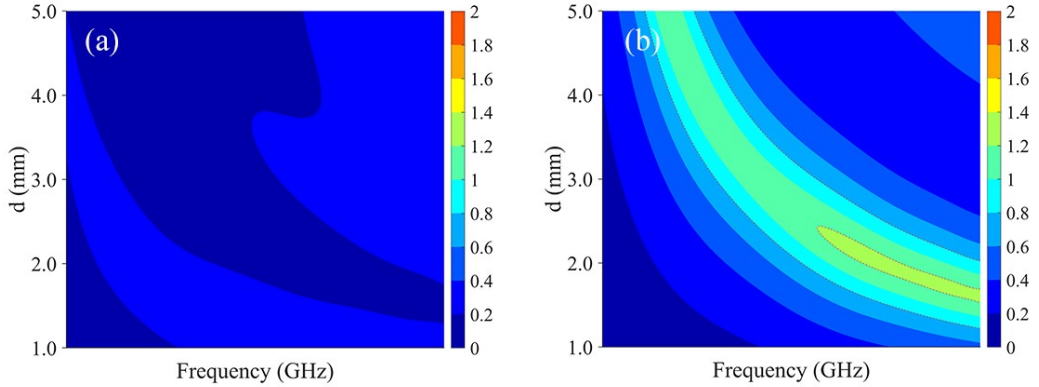

Fig. S6 2D contour maps of $|Z_{in}/Z_0|$ of (a) CNFs and (b) Fe_2P@CNFs.

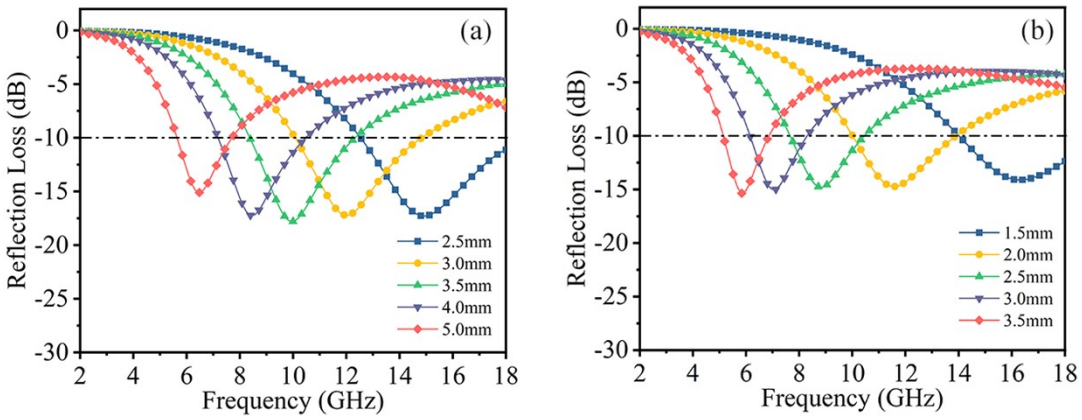

Fig. S7 RL curves at some specific thicknesses for the Fe_2P@CNFs/paraffin composites with filler loadings of (a) 7.5 wt% and (b) 12.5 wt%.

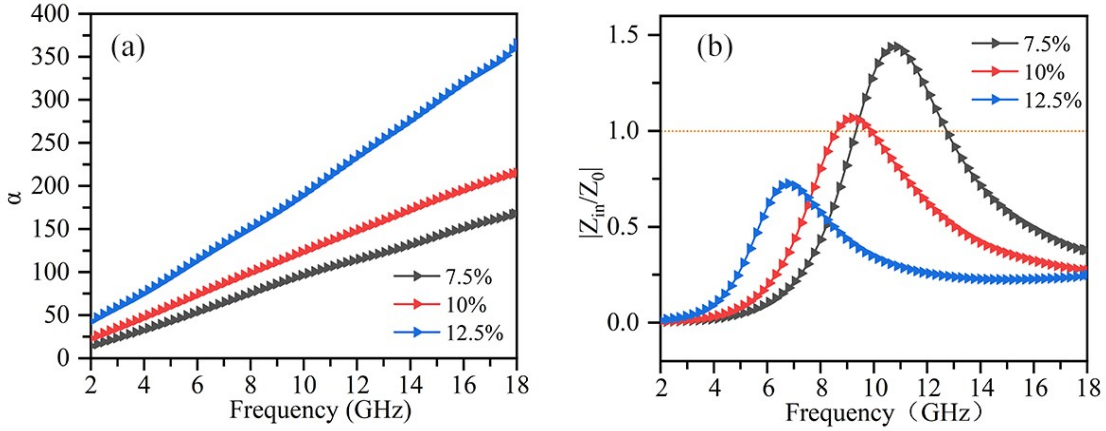

Fig. S8 Frequency dependence of (a) attenuation constant α and (b) impedance matching ratio $|Z_{in}/Z_0|$ of the Fe_2P@CNFs composites with different filler loadings (7.5, 10, and 12.5 wt%).

Table. S1 Microwave absorption properties of some representative transition metal phosphides and their composites.

Sample	Loading (wt%)	RL_{min} (dB)	EAB (GHz)	Ref.
Ni_2P/rGO	30	–38.3	3.8	[30]
NiCoP/rGO	50	–20.6	4.1	[14]
Ni/NiP@NC	40	−56.1	4.3	[31]
$Ni_{1-x}Co_xP$/MWNTs	25	–26.8	2.2	[32]
Ni-Co-P	40	–41.7	2.2	[33]
$Ni_{12}P_5/Ni_2P$	35	–50.06	3.3	[34]
Co_2P	60	–39.5	2.4	[13]
FeP	60	–37.7	2.8	[35]
Fe_2P@CNFs	10	–49.2	6.0	This work

Table. S2 Microwave absorption properties of some representative iron-based materials.

Sample	Loading (wt%)	RL_{min} (dB)	EAB (GHz)	Ref.
γ -Fe_2O_3@N-RGO	30	-41.1	3.4	[1]
RGO/γ-Fe_2O_3@C	20	-32.4	3.0	[2]
γ -Fe_2O_3@porous-RGO	17	-34.2	4.5	[3]
Fe-N@SiO_2	50	−23.1	2.4	[4]
$Fe_{70}Si_{30}$	75	-16.5	-	[5]
Fe/TiO_2 nanowire arrays	80	-28.36	1.36	[6]
FeCo@SiO_2@TiO_2	70	-33.72	5.8	[7]
Fe_2P@CNFs	10	–49.2	6.0	This work

References

1 J. Wang, J. Ren, Q. Li, Y. Liu, Q. Zhang and B. Zhang, *Carbon*, 2021, **184**, 195-206.

2 S. Ouyang, H. Fu, Y. Xie, W. He and Y. Ling, *Journal of Alloys and Compounds*, 2022, **920**, 166015.

3 S. Wang, Q. Jiao, X. Liu, Y. Xu, Q. Shi, S. Yue, Y. Zhao, H. Liu, C. Feng and D. Shi, *ACS Sustainable Chemistry & Engineering*, 2019, **7**, 7004-7013.

4 X. Kou, Y. Zhao, L. Xu, Z. Kang, Y. Wang, Z. Zou, P. Huang, Q. Wang, G. Su, Y. Yang and Y. Sun, *Journal of Colloid and Interface Science*, 2022, **615**, 685-696.

5 G. Xie, L. Yuan, P. Wang, B. Zhang, P. Lin and H. Lu, *Journal of Non-Crystalline Solids*, 2010, **356**, 83-86.

6 Y. Zhu, X. Li, P. Chen and B. Zhu, *Ceramics International*, 2020, **46**, 23985-23996.

7 Y. Li, H. Cheng, N. Wang, S. Zhou, D. Xie, T. Li, *J. Magn. Magn. Mater*, 2019, **471**, 346–354.